

# Calix[4]Arene and Calix[8]Arene Langmuir Films: Surface Studies, Optical and Structural Characterizations

Darvina Lim C.K, Faridah L. Supian

**Abstract:** In this work, the characterization of calix[4]arene (C4) and calix[8]arene (C8) were studied using Langmuir-Blodgett (LB) technique, surface potential meter and UV-Visible spectrometer. The surface pressure - area isotherms demonstrated stable Langmuir C4 and C8 monolayers formed at the air/water interface. Several properties such as limiting area per molecule and molecule radius of C4 and C8 were determined using different spreading volumes in LB technique. Besides that, effective dipole moments and maximum surface potential of C4 and C8 were determined from surface potential values. In addition, UV-Vis spectroscopy stated that the peak absorbance of C4 occurred at 275nm with one "shoulder" peak exists at 283nm, whilst peak absorbance of C8 occurred at 287nm. Surface topography for C4 and C8 thin layer also been observed. This study wasper formed to determine several basic properties of these calixarenes for future works.

**Keywords:** Calixarenes, Langmuir-Blodgett, surface potential, UV-Visible property

## I. INTRODUCTION

Calixarenes, the third generation of supramolecules [1] are a class of macrocyclic compounds. Calixarenes were first introduced in the year of 1872 by Adolph von Baeyer [2] before being studied extensively due to their substituted derivatives selective ionic and molecular-binding properties with others [3, 4]. Calixarenes have a well-established nomenclature for the family members where bracketed number, n is placed between the name calix and arene (i.e. calix[4]arene (C4) and calix[8]arene (C8) in this study) as to show the phenolic units that connected by alkylidene group to form their molecular cavity [2]. Generally calixarenes are amphiphilic molecules that consist of hydrophobic upper rim and hydrophilic lower rims that allowed them to form an insoluble monolayer on the air/water interface. Thus, Langmuir-Blodgett (LB) technique that allowed the self-assembly of calixarenes as Langmuir monolayers on the water surface is one of the suitable approaches to characterize these molecules [5]. In this report, we present the study on several basic properties of C4 and C8 through LB technique, surface potential probe, UV-Visible (UV-Vis) spectrometer and Field Emission Scanning Electron Microscope (FESEM).

**Revised Manuscript Received on May 22, 2019.**

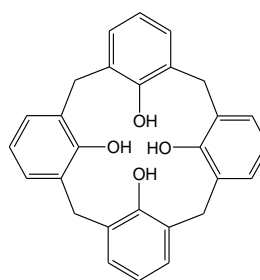
**Darvina Lim. C.K.**, Department of Physics, Faculty of Science and Mathematics, Sultan Idris Education University (UPSI), 35900 Tanjong Malim, Perak, Malaysia.

**Faridah L. Supian**, Department of Physics, Faculty of Science and Mathematics, Sultan Idris Education University (UPSI), 35900 Tanjong Malim, Perak, Malaysia.

This study was conducted to get some understanding about the calixarene behavior on the air-water interface and also the formation of the calixarene LB thin film.

## II. MATERIALS AND METHOD

(a)



(b)

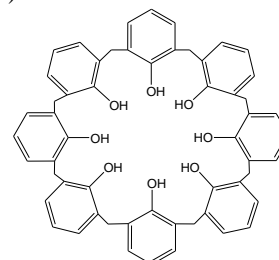


**Fig. 1 Molecular structure of (a) C4 (C<sub>28</sub>H<sub>24</sub>O<sub>4</sub>) and (b) C8 (C<sub>56</sub>H<sub>48</sub>O<sub>8</sub>)**

Main materials in this study are 25, 26, 27, 28-tetrahydrocalix[4]arene (C4) and 49, 50, 51, 52, 53, 54, 55, 56-octahydrocalix[8]arene (C8) (FIGURE 1) that purchased from Sigma-Aldrich. Each of the calixarenes was dissolved in chloroform (CHCl<sub>3</sub>) to produce 0.2 mg/ml of calixarene solution. The calixarenes and their organic solvent, CHCl<sub>3</sub> (>99.8% purity) were used without additional purification procedure. Pieces of quartz with a dimension of 2.5 cm × 2.5 cm were selected as the substrate for calixarene LB thin film deposition. Proper cleaning method was utilized to ensure the cleanliness of the substrate. Initially, the substrates were cleaned with Decon 90 before rinsed with deionized (DI) water. Later, ultrasonication (40 kHz) of substrates with the sequences of acetone (10 minutes), DI water (2 minutes), propanol (10 minutes) and DI water (2 minutes) again before the drying process with a nitrogen gun take place. Finally, the substrates were being treated hydrophobically with 1,1,1,3,3,3-Hexamethyldisilazane (C<sub>6</sub>H<sub>19</sub>NSi<sub>2</sub>) overnight to improve the attachment of calixarene LB monolayer on the substrates.

### III. CHARACTERIZATION

The surface pressure-area ( $\Pi$ -A) isotherms of calixarenes were measured on a medium-sized KSV NIMA 2002 System 2 LB deposition trough (sensitivity =  $\pm 0.001$  mN/m). The filter paper was used as the pressure sensor to detect surface pressure changes exerted by the monolayer. Deionized water with 18.2 M $\Omega$ -cm resistivity, produced from Merck Millipore water system was poured into the trough as the subphase. Before the measurement was performed, the cleanliness of water surface was ensured free from dust and foreign particles through micro-aspiration.

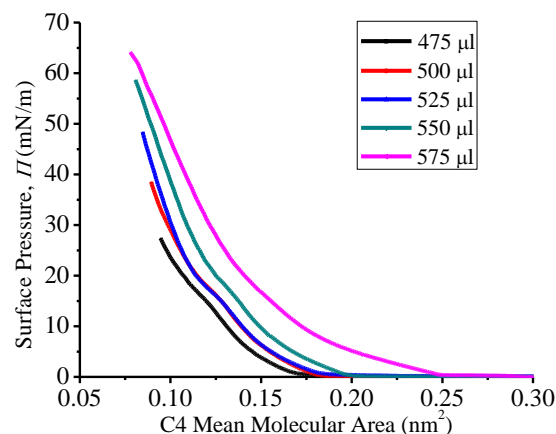
For the  $\Pi$ -A isotherm measurement, a SGE Analytical Science Microlitre Syringe was utilized to spread dropwise the calixarene solution uniformly on the water subphase. The solvent of the calixarene solution was allowed to evaporate for about 20 minutes before the measurement was taken. This is a necessary stage as to allow only calixarene molecules on the air/water subphase. Finally, the calixarene molecules were symmetrically compressed into a rigid monolayer by both barriers using a speed of 12 mm/min.

As for the surface potential-area ( $\Delta V$ -A) measurement, a KSV SPOT probe (sensitivity = 1 mV) that used vibrating plate capacitor method was utilized. A counter electrode that made up of stainless steel plate was placed under the monolayer whilst the vibrating plate was located about 1 mm above the monolayer. The KSV software in a computer collected both the surface pressure and surface potential data simultaneously.  $\Pi$ -A isotherm and  $\Delta V$ -A isotherm graphs were plotted from the data using OriginLab. Standard trough cleaning practice was applied between different spreading volume measurements of calixarenes.

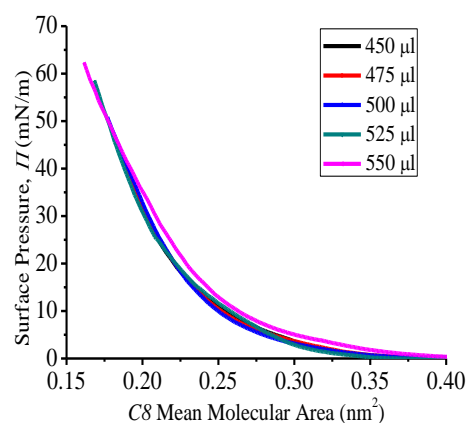
Both, C4 and C8 monolayer were attached on the quartz substrate through vertical dipping method in LB trough to form 9 layers of Y-type LB deposition thin film. Deposition pressure of 30 mN/m was applied for the monolayer as at this specific pressure, the monolayer has started to develop a solid-like state. Upward and downward dipping stroke speeds of 5 mm/min were used with a drying period of 10 minutes for the thin film. The work using LB technique has been carried out in a constant temperature cleanroom ( $22 \pm 1$  °C). Several optical properties of the C4 and C8 were characterized using an Agilent 8453 UV-Vis Spectroscopy with a 1cm path length of the cuvette for the solution analysis. The calixarene solutions have a serial dilution from 0.10 mg/ml to 0.02 mg/ml with a decrement of 0.02 mg/ml since the more diluted solution has less noise on the absorbance spectra. The surface topography of the thin films also being observed using FESEM in different magnification scale.

### IV. RESULTS AND DISCUSSION

#### Surface Pressure-Area ( $\Pi$ -A), Surface Potential-Area ( $\Delta V$ -A) and Effective Dipole Moment-Area ( $\mu$ -A) Isotherms



(a)



(b)

**Fig. 2  $\Pi$ -A isotherm graphs for (a) C4 and (b) C8**

From the  $\Pi$ -A isotherm graph in FIGURE 2, C4 and C8 monolayers were studied through the surface pressure as a function of the molecular area at the air/water surface. The hydrophilic hydroxyl group ( $-OH$ ) of both calixarenes that bonded at phenol units are assumed to be in the water subphase and the hydrophobic aromatic hydrocarbon groups are estimated to be in contact with the air [6].

From the FIGURE 2, the  $\Pi$ -A isotherm curve of C4 is being shifted to the right, while the  $\Pi$ -A isotherm curve of C8 remains almost the same position. These result from the different in intermolecular packing structure among the molecule on air/water interface [7]. Both the  $\Pi$ -A isotherm curve of C4 and C8 have demonstrated the same pattern of phase transition curve from a gaseous state to liquid-expanded state, followed by liquid-condensed state and lastly the solid state. The experimental mean molecular areas of both calixarenes were determined through extrapolation of the linear region of the isotherm curves to zero surface pressure.

Then, the experimental radius (TABLE 1 and 2) of both, C4 and C8 molecules were calculated using the formula that related to the cross sectional area of a circle.

**Table. 1 Data from  $\Pi$ -A isotherm graphs for C4 Langmuir monolayer**

Volume ( $\mu$ l)	Mean molecular area (nm <sup>2</sup> )	Radius (nm)
475	0.135	0.207
500	0.134	0.207
525	0.127	0.201
550	0.139	0.210
575	0.157	0.224

**Table. 2 Data from  $\Pi$ -A isotherm graphs for C8 Langmuir monolayer**

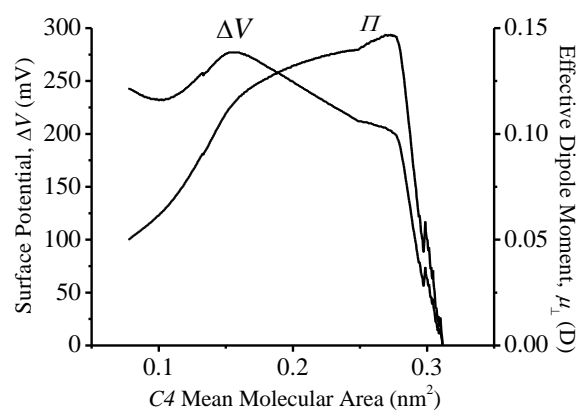
Volume ( $\mu$ l)	Mean molecular area (nm <sup>2</sup> )	Radius (nm)
450	0.251	0.283
475	0.237	0.275
500	0.242	0.278
525	0.232	0.272
550	0.250	0.282

From the TABLES 1 and 2, the experimental mean molecular area of C4 almost twice smaller than C8. The nm<sup>2</sup> and 0.27 nm.

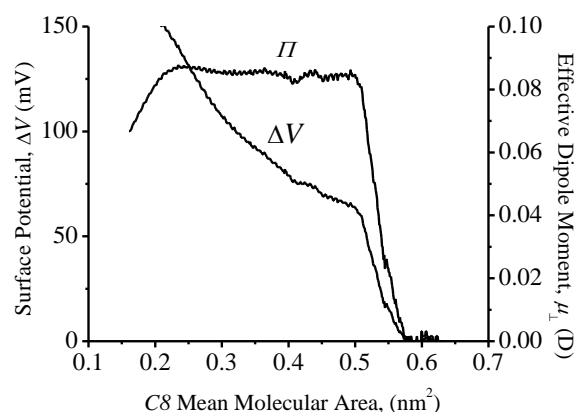
Next, the electrical structure of the calixarene monolayer surfaces was studied through the value of  $\Delta V$  as a function of the molecular area at the air/water interface. In this study,  $\Delta V$  is the potential difference between the surface of calixarene monolayer and the surface of clean water subphase [8]. Later, by using Helmholtz equation (1) as shown below, the average effective dipole moment ( $\mu_{\perp}$ ) of calixarene monolayer molecule was calculated from the  $\Delta V$  values as shown below:

$$\mu_{\perp} = \epsilon_0 \epsilon_r A \Delta V \quad (1)$$

which  $\mu_{\perp}$  is the average effective dipole moment of calixarene monolayer molecule,  $\epsilon_0$  is the free space permittivity ( $8.854 \times 10^{-12} \text{ C}^2 \text{N}^{-1} \text{m}^{-2}$ ), while  $\epsilon_r$  is the relative permittivity for the monolayer between the electrodes and A is the area per molecule in m<sup>2</sup>. The value of  $\epsilon_r$  is estimated as 1 since the air gap that exists between the vibrating plate and the calixarene monolayer is large as compared to the monolayer thickness itself [9]. The calculated  $\mu_{\perp}$  values, stated in Debye unit (D) were used to plot the curve of  $\mu_{\perp}$  as a function of the molecular area at the air/water interface. The maximum  $\Delta V$  ( $\Delta V_{\max}$ ) value was obtained from the position of the maximum  $\mu_{\perp}$  ( $\mu_{\perp \max}$ ) value when both curves,  $\Delta V$ -A and  $\mu_{\perp}$ -A were plotted on the same graph. One of the  $\Delta V$  and  $\mu_{\perp}$  graphs for each C4 and C8 with spreading volume of 575  $\mu$ l and 550  $\mu$ l respectively are shown in FIGURE 3. All the data obtained were tabulated in TABLE 3.



(a) 575  $\mu$ l of C4



(b) 550  $\mu$ l of C8

**Fig. 3  $\Delta V$ -A and  $\mu_{\perp}$ -A isotherm graphs for (a) 575  $\mu$ l of C4 and (b) 550  $\mu$ l of C8**

**Table. 3 Data from  $\Delta V$ -A and  $\mu_{\perp}$ -A isotherm graphs for C4 and C8 Langmuir monolayer**

C4			C8		
Volume ( $\mu$ l)	$\Delta V_{\max}$ (mV)	$\mu_{\perp \max}$ (D)	Volume ( $\mu$ l)	$\Delta V_{\max}$ (mV)	$\mu_{\perp \max}$ (D)
475	223	0.090	450	66	0.103
500	203	0.090	475	121	0.071
525	172	0.104	500	205	0.132
550	183	0.110	525	120	0.070
575	205	0.147	550	141	0.088

For C4, the  $\Delta V_{\max}$  values and  $\mu_{\perp \max}$  values for all spreading volumes are closer to each other, but the  $\Delta V_{\max}$  values and  $\mu_{\perp \max}$  values for C8 are much more differ from each other. These  $\Delta V_{\max}$  values and  $\mu_{\perp \max}$  values are contributed by the interaction between calixarene molecules that interact with each other and caused the uplifting of their hydrophobic part with respect to the horizontal direction of the subphase as the compression of the monolayer took place [10].

### UV-Visible (UV-Vis) Absorbance Results

The UV absorption of the *C4* and *C8* solutions with different dilution were illustrated in FIGURE 4. *C4* has peak absorbance occurred at 275 nm with one “shoulder” peak exists at 283 nm, whereas *C8* has peak absorbance occurred at 287nm. The peaks are attributed to  $\pi$ - $\pi^*$  and  $n$ - $\pi^*$  transition [11, 12]. Another peak of both *C4* and *C8* solutions that occurred below 245 nm will not be considered as the absorbance peak since  $\text{CHCl}_3$  has a “cut-off” wavelength below 245 nm for a 1cm path length of the cuvette [13].

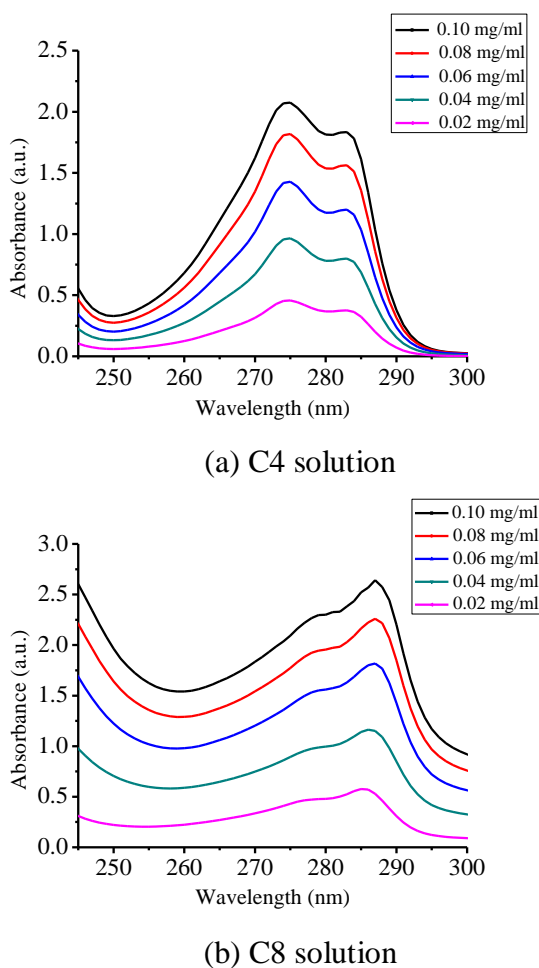
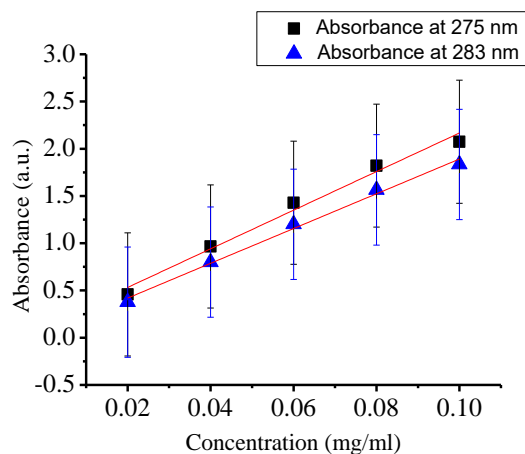


**Fig. 4** UV-Vis absorbance spectra of (a) *C4* solution and (b) *C8* solution with different concentration

By using the Beer-Lambert Law (2), the molar absorptivity of *C4* and *C8* were calculated for each absorbance peaks and the “shoulder” peak as demonstrated in FIGURE 5 and TABLE 4:

$$\varepsilon = \frac{A}{bc} \quad (2)$$

where  $\varepsilon$  is the molar absorptivity ( $\text{Lmol}^{-1}\text{cm}^{-1}$ ),  $A$  is the absorbance,  $b$  is the solution path length (1 cm in this study) for the light to travel and  $c$  is the concentration of the solution ( $\text{molL}^{-1}$ ). The absorbance data plotted in FIGURE 5 has error bars indicating standard deviation around the mean.



(a) *C4* solution

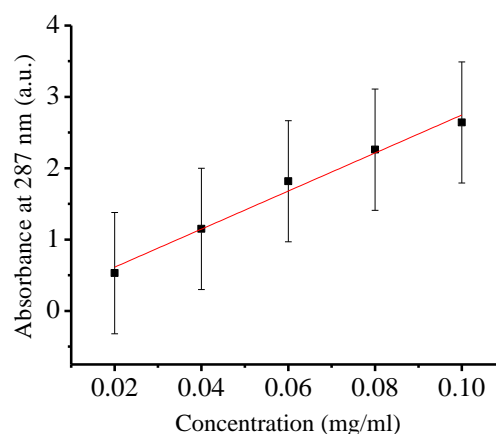


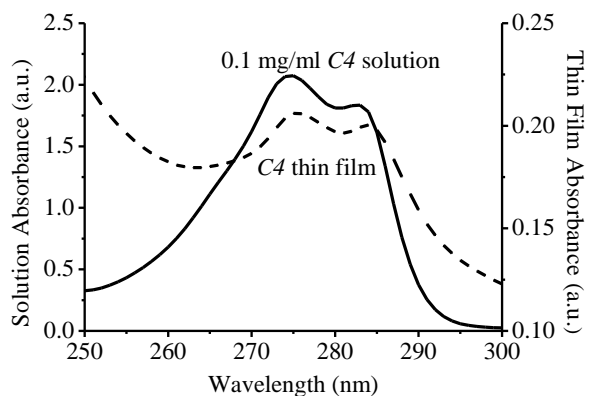
**Fig. 5** UV-Vis Absorbance versus Concentration of (a) *C4* solution and (b) *C8* solution

**Table. 4** Molar Absorptivity of *C4* and *C8* solution

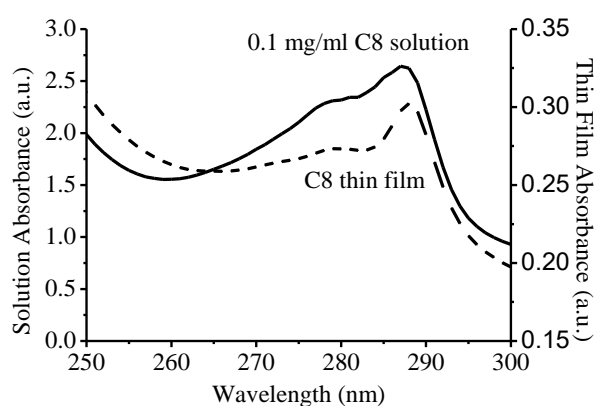
C4solution		C8solution	
Absorbance Peak (nm)	Molar Absorptivity ( $\text{Lmol}^{-1}\text{cm}^{-1}$ )	Absorbance Peak (nm)	Molar Absorptivity ( $\text{Lmol}^{-1}\text{cm}^{-1}$ )
275	8677	287	22643
283	7811		

LB thin film of both calixarenes that deposited on quartz was analyzed using UV-Vis spectrometer and compared with their solution UV-Vis spectra as display in FIGURE 6. The peak absorbance of *C4* thin film occurred at 275 nm with a slightly red shift in the “shoulder” peak at 284 nm. The peak absorbance of *C8* thin film displayed at 288 nm with a slightly red shift in the peak wavelength as compared to its’ solution absorbance peak. Both calixarene thin films still retained their fingerprint absorbance peak although being deposited as thin film indicated their stability in solid form.





(a)

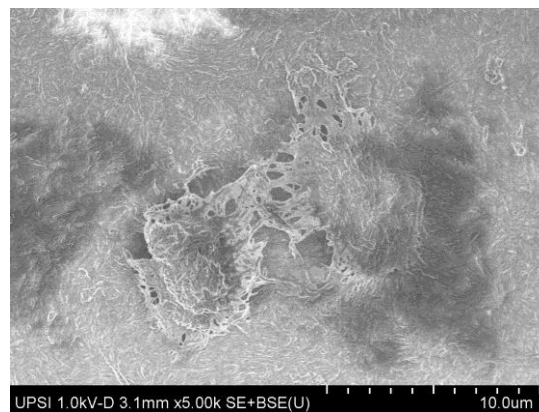
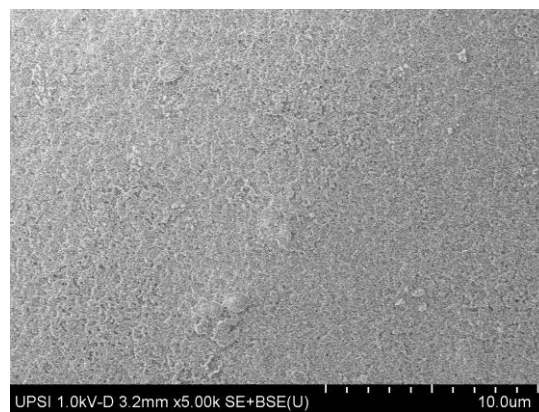


(b)

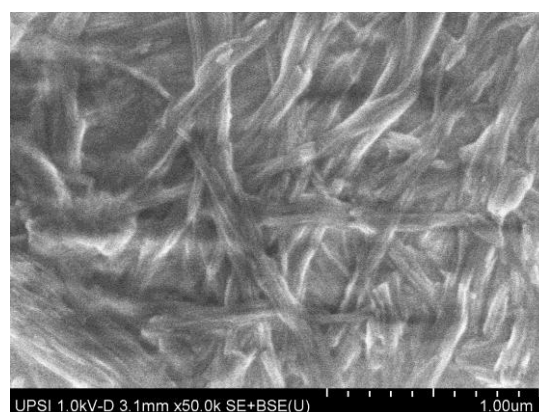
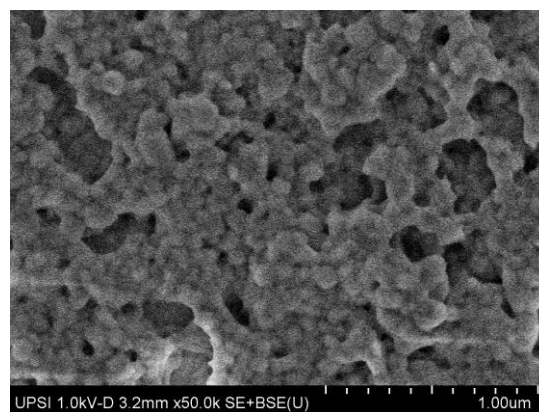
**Fig. 6 UV-Vis absorbance spectra of (a) C4 solution and thin film; (b) C8 solution and thin film**

#### Surface Topography Analysis

The topography of the C4 and C8 thin film were studied using FESEM as shown in FIGURE 7 below. Generally, both thin film display rather uniform top view surface under low FESEM magnification. Certain areas on the thin film display mountain-like structure. These are contributed by the insufficient space during the drying up process[14] and had been described in the previous paper [15]. Zoomed-in view reveals that the C4 molecules exist in irregular sphere shape and close to each other with some spaces between the molecules. As for C8 zoomed-in view, the diagram reveal that C8 molecules exist in irregular needle-shape and arrange randomly on top of each other. Overall, the thin film for both calixarenes still rather uniform using the Langmuir-Blodgett technique.



(a)



(b)

**Fig. 7 Surface morphology of (a) C4 thin film and (b) C8 thin film deposited on quartz**

## V. CONCLUSION

Several characteristics of C4 and C8 were analyzed using LB technique,  $\Delta V$  probe, UV-Vis spectroscopy and FESEM. From the LB method,  $\Pi$ -A,  $\Delta V$ -A and  $\mu$ -A isotherm were studied. The UV-Vis absorbance peak of C4 and C8 in solution and the thin film also determined to study the suitability of these calixarenes to be deposited in solid form. Molar absorptivity for the calixarene absorbance peaks also being studied. The surface topography of C4 and C8 thin films demonstrated almost uniform surface area. The thin film and solution of C4 and C8 can be further studied to investigate the potential application, especially in aqueous ion sensing.

## ACKNOWLEDGMENTS

Financial support from RACE Research Grant (0003-102-62), UPSI and MOHE were acknowledged with gratitude. Instrumentation facilities provided by the Physics Department and Chemistry Department, UPSI are gratefully acknowledged.

## REFERENCES

1. G. Yu, K. Jie and F. Huang, Chem. Rev.115, 7240–7303 (2015). doi:10.1021/cr5005315
2. O. Gezici and M. Bayrakci, J. Incl. Phenom. Macro.83, 1-18 (2015).doi:10.1007/s10847-015-0553-4
3. Q. Yang,X. Qin, C. Yan, and X. Zhu, Sensor Actuat. B-Chem.212, 183-189 (2015). doi: 10.1016/j.snb.2015.02.020
4. R. Chester, et al, Anal. Chim. Acta 851, 78-86 (2014). doi:10.1016/j.aca.2014.08.046
5. L. G. Tulli, et al, Langmuir31, 2351-2359 (2015). doi:10.1021/acs.langmuir.5b00262
6. W. He, D. Vollhardt, R. Rudert, L. Zhu, and J. Li, Langmuir 19, 385-392 (2003). doi:10.1021/la020714i
7. Dhanabalan, L. Gaffo, A. M. Barros, W. C. Moreira, and O. N. Oliveira, Langmuir 15, 3944-3949 (1999).doi:10.1021/la9815188
8. F. L. Supian, et al, Langmuir 26, 10906–10912 (2010).doi:10.1021/la100808r
9. B. Korchowiec, et al, J. Phys. Chem. B 111, 13231-13242 (2007). doi:10.1021/jp070970+
10. Bauman, A. Plóciennik and K. Inglot, Acta Phys. Pol. A116(2), 203-210 (2009). doi:10.12693/APhysPolA.116.203
11. M. Ignat, A. Farcas, A. Vasile and E. Popovici, Stud. Surf. Sci. Catal. 174A, 389–392 (2008). doi: 10.1016/S0167-2991(08)80224-8
12. M. Kobayashi, et al, Opt. Express 20, 24856-24863 (2012).doi:10.1364/OE.20.024856.
13. N. V. Tkachenko, Optical Spectroscopy Methods and Instrumentations, Oxford: Elsevier, 2006, pp. 299.
14. M. M. Jaafar, et al. Langmuir31(38), 10426–10434 (2015).doi:10.1021/acs.langmuir.5b02708
15. L. C. K. Darvina and L. S. Faridah, Jurnal Fizik Malaysia38, 10034-10043 (2017).